Parametric coherent receiver

Citation for the original published paper (version of record):
Kumpera, A., Malik, R., Lorences Riesgo, A. et al (2015). Parametric coherent receiver. Optics Express, 23(10): 12952-12964. http://dx.doi.org/10.1364/oe.23.012952

Parametric coherent receiver

Aleš Kumpera, Rohit Malik, Abel Lorences-Riesgo, and Peter A. Andrekson*

Fibre Optic Communication Research Centre (FORCE), Photonics Laboratory, Department of Microtechnology and Nanoscience, Chalmers University of Technology, Gothenburg 412 96, Sweden

*peter.andrekson@chalmers.se

Abstract: We present the parametric coherent receiver based on a two-mode pump-degenerate fiber optical parametric amplifier (FOPA). The receiver is inherently single-ended and offers a simultaneous gain and coherent mixing of the received signal and a reference wave (known as a local oscillator signal) with, in principle, arbitrary wavelength separation. We analyze the receiver theoretically and in a proof-of-concept experiment. As a reference we compare the performance to a standard single-ended homodyne coherent receiver.

OCIS codes: (060.1660) Coherent communications; (190.4970) Parametric amplifiers and oscillators; (190.4380) Nonlinear optics, four-wave mixing.

References and links

1. R. Linke and A. Gnauck, "High-capacity coherent lightwave systems," J. Lightwave Technol. **6**, 1750–1769 (1988).
2. O. Lidoyne, P. Gallion, and D. Erasme, "Analysis of a homodyne receiver using an injection-locked semiconductor laser," J. Lightwave Technol. **9**, 659–665 (1991).
3. K. Kikuchi, "Proposal and performance analysis of novel optical homodyne receiver having an optical preamplifier for achieving the receiver sensitivity beyond the shot-noise limit," IEEE Photon. Technol. Lett. **4**, 195–197 (1992).
4. P. Johannisson, M. Sjodin, M. Karlsson, E. Tipsuwannakul, and P. Andrekson, "Cancellation of nonlinear phase distortion in self-homodyne coherent systems," IEEE Photon. Technol. Lett. **22**, 802–804 (2010).
5. T. Miyazaki and F. Kubota, "PSK self-homodyne detection using a pilot carrier for multibit/symbol transmission with inverse-RZ signal," IEEE Photon. Technol. Lett. **17**, 1334–1336 (2005).
6. L. G. Kazovsky, "Decision-driven phase-locked loop for optical homodyne receivers: Performance analysis and laser linewidth requirements," J. Lightwave Technol. **3**, 1238–1247 (1985).
7. T. Pfau, S. Hoffmann, and R. Noé, "Hardware-efficient coherent digital receiver concept with feedforward carrier recovery for M-QAM constellations," J. Lightwave Technol. **27**, 989–999 (2009).
8. S. K. Ibrahim, S. Sygletos, R. Weerasuriya, and A. D. Ellis, "Novel real-time homodyne coherent receiver using a feed-forward based carrier extraction scheme for phase modulated signals," Opt. Express **19**, 8320–8326 (2011).
9. G. Abbas, V. W. S. Chan, and T. Yee, "A dual-detector optical heterodyne receiver for local oscillator noise suppression," J. Lightwave Technol. **3**, 1110–1122 (1985).
10. Y. Painchaud, M. Poulin, M. Morin, and M. Têtu, "Performance of balanced detection in a coherent receiver," Opt. Express **17**, 3659–3672 (2009).
11. M. Seimetz, "Phase diversity receivers for homodyne detection of optical DQPSK signals," J. Lightwave Technol. **24**, 3384–3391 (2006).
12. K. Kikuchi and S. Tsukamoto, "Evaluation of sensitivity of the digital coherent receiver," J. Lightwave Technol. **26**, 1817–1822 (2008).
13. J. Hansryd, P. A. Andrekson, M. Westlund, J. Li, and P. Hedekvist, "Fiber-based optical parametric amplifiers and their applications," IEEE J. Sel. Top. Quantum Electron. **8**, 506–520 (2002).
14. M. E. Marhic, P. A. Andrekson, P. Petropoulos, S. Radic, C. Peucheret, and M. Jazayerifar, "Fiber optical parametric amplifiers in optical communication systems," Las. Photon. Rev. 1–25 (2014).
15. J. Hansryd and P. A. Andrekson, "Broad-band continuous-wave-pumped fiber optical parametric amplifier with 49-db gain and wavelength-conversion efficiency," IEEE Photon. Technol. Lett. **13**, 194–196 (2001).

#233505 - $15.00 USD Received 29 Jan 2015; revised 24 Mar 2015; accepted 30 Mar 2015; published 8 May 2015

16. R. Jiang, R. Saperstein, N. Alic, M. Nezhad, C. McKinstrie, J. Ford, Y. Fainman, and S. Radic, "Parametric wavelength conversion from conventional near-infrared to visible band," IEEE Photon. Technol. Lett. **18**, 2445–2447 (2006).
17. F. Gholami, B. P.-P. Kuo, S. Zlatanovic, N. Alic, and S. Radic, "Phase-preserving parametric wavelength conversion to SWIR band in highly nonlinear dispersion stabilized fiber," Opt. Express **21**, 11415–11424 (2013).
18. C. McKinstrie and S. Radic, "Phase-sensitive amplification in a fiber," Opt. Express **12**, 4973–4979 (2004).
19. Z. Tong, C. Lundström, P. A. Andrekson, C. J. McKinstrie, M. Karlsson, D. J. Blessing, E. Tipsuwannakul, B. J. Puttnam, H. Toda, and L. Grüner-Nielsen, "Towards ultrasensitive optical links enabled by low-noise phase-sensitive amplifiers," Nat. Photonics **5**, 430–436 (2011).
20. R. Malik, A. Kumpera, S. L. I. Olsson, P. A. Andrekson, and M. Karlsson, "Optical signal to noise ratio improvement through unbalanced noise beating in phase-sensitive parametric amplifiers," Opt. Express **22**, 10477–10486 (2014).
21. N. A. Olsson, "Lightwave systems with optical amplifiers," J. Lightwave Technol. **7**, 1071–1082 (1989).
22. C. Crognale, "Sensitivity and power budget of a homodyne coherent DP-QPSK system with optical amplification and electronic compensation," J. Lightwave Technol. **32**, 1295–1306 (2014).
23. C. McKinstrie, S. Radic, and M. Raymer, "Quantum noise properties of parametric amplifiers driven by two pump waves," Opt. Express **12**, 5037–5066 (2004).
24. Z. Tong, A. Bogris, C. Lundström, C. J. McKinstrie, M. Vasilyev, M. Karlsson, and P. A. Andrekson, "Modeling and measurement of the noise figure of a cascaded non-degenerate phase-sensitive parametric amplifier," Opt. Express **18**, 14820–14835 (2010).
25. P. Kylemark, P.-O. Hedekvist, H. Sunnerud, M. Karlsson, and P. A. Andrekson, "Noise characteristics of fiber optical parametric amplifiers," J. Lightwave Technol. **22**, 409–416 (2004).
26. P. Kylemark, M. Karlsson, and P. A. Andrekson, "Gain and wavelength dependence of the noise-figure in fiber optical parametric amplification," IEEE Photon. Technol. Lett. **18**, 1255–1257 (2006).
27. R. Malik, S. Olsson, P. A. Andrekson, C. Lundström, and M. Karlsson, "Record-high sensitivity receiver using phase sensitive fiber optical parametric amplification," in "Optical Fiber Communication Conference (OFC 2014), paper Th2A.54," (2014).
28. C. Lundström, R. Malik, L. Gruner-Nielsen, B. Corcoran, S. L. I. Olsson, M. Karlsson, and P. A. Andrekson, "Fiber optic parametric amplifier with 10-db net gain without pump dithering," IEEE Photon. Technol. Lett. **25**, 234–237 (2013).
29. A. Lorences-Riesgo, L. Liu, S. L. I. Olsson, R. Malik, A. Kumpera, C. Lundström, S. Radic, M. Karlsson, and P. A. Andrekson, "Quadrature demultiplexing using a degenerate vector parametric amplifier," Opt. Express **22**, 29424–29434 (2014).
30. S. L. I. Olsson, B. Corcoran, C. Lundström, E. Tipsuwannakul, S. Sygletos, A. D. Ellis, Z. Tong, M. Karlsson, and P. A. Andrekson, "Injection locking-based pump recovery for phase-sensitive amplified links," Opt. Express **21**, 14512–14529 (2013).
31. E. Myslivets, B. P. Kuo, N. Alic, and S. Radic, "Generation of wideband frequency combs by continuous-wave seeding of multistage mixers with synthesized dispersion," Opt. Express **20**, 3331–3344 (2012).

1. Introduction

Optical coherent detection is a well-known and mature technique that enables detection of optical signals with enhanced sensitivity [1]. Before the era of optical amplifiers (rare-earth-doped and Raman amplifiers) it represented a method for overcoming the photodetector thermal noise and how to achieve detection of low-intensity shot noise-limited signals. Not only had it impact on sensitivity but it also made detection of signals bearing phase-encoded information in non-differential modulation formats possible. In today's optical systems both features play an irreplaceable role.

In its basic form the coherent receiver comprises a two-input optical mixer and a single photodetector [1] (so-called single-ended option). One of the two input waves is the received signal which carries the information and the second one is a continuous wave (CW) acting as a reference signal. Both are coupled together in the optical mixer (e.g., optical coupler) and subsequently detected in the photodetector. The fundamental condition for coherent receivers is that the wavelength separation of both waves must fall within the receiver electrical bandwidth. The properties of the reference signal (commonly referred to as a local oscillator signal, LO) in respect to the received signal define the type of coherent detection. In homodyne detection [2, 3] the LO is frequency-locked to the carrier of the signal. To satisfy such condition

#233505 - $15.00 USD Received 29 Jan 2015; revised 24 Mar 2015; accepted 30 Mar 2015; published 8 May 2015

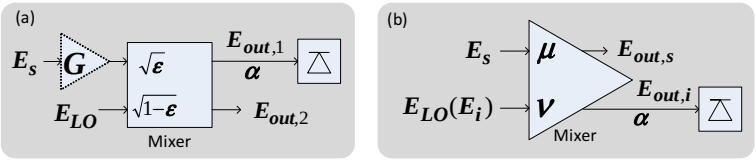

Fig. 1. Standard (a) and parametric (b) single-ended coherent receiver schemes.

either both signals are derived from the same laser source (signals split before modulation) and co-propagate in different channels, e.g., polarization-multiplexed channel [4, 5], or the LO is generated locally at the receiver's side which requires a complex phase-locked loop system [6]. Intradyne detection uses a free-running laser for the LO and its frequency is tuned close to the signal carrier frequency. The frequency difference of both signals is constantly tracked and compensated for after detection using digital signal processing (DSP) algorithms [7]. Systems where the incoming signal is processed to acquire a phase-locked LO have also been studied such as technique based on an extraction of the LO via modulation stripping [8]. Generally, coherent receivers demand LOs being high-power and low-noise laser sources. Satisfying both requirements is not trivial as lasers suffer from relative intensity noise (RIN). In case of single-ended coherent detection the RIN hinders the overall performance substantially [9], however, it can be partially suppressed via balanced coherent detection scheme [9, 10]. Since coherent receivers with only one reference signal are capable of detecting only a single-quadrature modulated signal thus more advanced modulation formats require a phase diversity concept [11, 12]. The concept takes advantage of two LOs shifted in phase by 90 degrees apart and mixed separately with the split input signal, thus covering both real and imaginary parts of the optical field. Besides coherent receivers can exploit optical amplification for a preamplification of the received signal which improves sensitivity and relaxes LO power demands [12].

In analogy to the single-ended homodyne coherent receiver (we refer to it as a standard coherent receiver, SCR) we present and study, for the first time to the best of our knowledge, a single-ended single-quadrature parametric coherent receiver (PCR) based on fiber optical parametric amplifier (FOPA). FOPAs, based on the nonlinear four-wave mixing (FWM) effect, have already proven themselves as promising devices for future optical transmission systems [13, 14] thanks to their high gain [15] and wideband nature [16, 17]. Coherent properties of FOPAs offer phase-sensitive operation [18] which can be harnessed, e.g., for an ultra-low-noise amplification [19] or for optical signal-to-noise-ratio (OSNR) improvement [20]. Here, from a coherent detection perspective, the FOPA serves as a coherent mixer and a preamplifier at the same time. The output signal is subsequently detected in a photodetector identically to the SCR. The approach offers unique detection capability through inherent gain for the received signal and the LO and through their coherent mixing while being, in principle, arbitrarily separated in wavelength (in contrast to conventional coherent receivers).

In this work, we theoretically analyze and perform a proof-of-concept experiment of the proposed PCR based on two-mode pump-degenerate FOPA and compare it to an SCR. We carry out bit-error-rate (BER) tests to compare the sensitivity performance both for intensity- (on-off keying, OOK) and for phase-modulated (binary phase-shift keying, BPSK) signals and point out performance penalties.

2. Concept

To give an intuitive insight into the presented PCR we review its theoretical background similar to the SCR (Fig. 1). The SCR with a preamplifier can be described via the two-port input-output

#233505 - $15.00 USD Received 29 Jan 2015; revised 24 Mar 2015; accepted 30 Mar 2015; published 8 May 2015

relation

$$\begin{bmatrix} E_{out,1} \\ E_{out,2} \end{bmatrix} = \begin{bmatrix} i\sqrt{\varepsilon} & \sqrt{1-\varepsilon} \\ \sqrt{1-\varepsilon} & i\sqrt{\varepsilon} \end{bmatrix} \begin{bmatrix} \sqrt{G}E_s \\ E_{LO} \end{bmatrix}, \tag{1}$$

where E_s is the complex optical field of the received signal, E_{LO} is the complex optical field of the LO, ε is the coupling coefficient, $E_{out,1}$ is the optical field at the output port 1 and $E_{out,2}$ at the output port 2, G is the preamplifier gain and $i^2 = -1$. The mixer output optical powers are

$$P_{out,1} = |E_{out,1}|^2 = \varepsilon G P_s + (1-\varepsilon)P_{LO} + 2[\varepsilon(1-\varepsilon)GP_sP_{LO}]^{1/2}\cos\Delta\varphi_{SCR}, \tag{2}$$

$$P_{out,2} = |E_{out,2}|^2 = \varepsilon G P_s + (1-\varepsilon)P_{LO} - 2[\varepsilon(1-\varepsilon)GP_sP_{LO}]^{1/2}\cos\Delta\varphi_{SCR}, \tag{3}$$

where $P_s = |E_s|^2$ and $P_{LO} = |E_{LO}|^2$. The phase relation between the signal and the LO is defined through $\Delta\varphi_{SCR} = \varphi_s - \varphi_{LO} + \pi/2$ where φ_s is the phase angle of the signal and φ_{LO} is the phase angle of the LO. It is assumed that both signals are co-polarized. Since P_{LO} is a CW and in most cases $P_{LO} \gg P_s$ the generated photocurrent has two components. The first one is proportional to the first two terms in Eqs. (2) and (3) which is in principle just a photocurrent offset. The second one, i_{det}, is proportional to the third mixing term and carries the information from the received signal. For the following discussion we assume the signal and the LO are phase-locked, $\Delta\varphi_{SCR} = 0$. The signal-to-noise ratio (SNR) of the detected signal is defined as

$$SNR = \frac{\langle i_{det}^2 \rangle}{\sigma^2}, \tag{4}$$

where $\langle i_{det}^2 \rangle$ stands for the average photocurrent power and σ^2 is the average noise power (the photocurrent variance). The SNR of the SCR with preamplifier is then defined as

$$SNR_{SCR} = \frac{4R_s^2\alpha^2\varepsilon(1-\varepsilon)GP_sP_{LO}}{\sigma_{det}^2 + \sigma_s^2 + \sigma_{LO}^2 + \sigma_{LO-RIN}^2 + \sigma_{ASE}^2 + \sigma_{S-ASE}^2 + \sigma_{LO-ASE}^2 + \sigma_{ASE-ASE}^2}, \tag{5}$$

where R_s is the photodetector responsivity at the signal frequency, α is the additional loss between the mixer and the photodetector, σ_{det}^2 is the photodetector circuit noise variance, σ_s^2 is the signal shot noise variance, σ_{LO}^2 is the LO shot noise variance and σ_{LO-RIN}^2 is the LO relative intensity noise (RIN) variance, σ_{ASE}^2 is the amplified spontaneous emission (ASE) shot noise variance. The other variances stem from beatings between the signal and the ASE, σ_{S-ASE}^2, between the LO and the ASE, σ_{LO-ASE}^2, and between the ASE itself, $\sigma_{ASE-ASE}^2$. The variances and their definitions are well-established in the field of coherent receivers [21, 22]. In our study we define them as

$$\sigma_{det}^2 = \frac{4k_BTF_{det}}{R_L}B_e \tag{6}$$

$$\sigma_s^2 = 2qR_s\alpha\varepsilon GP_sB_e \tag{7}$$

$$\sigma_{LO}^2 = 2qR_s\alpha(1-\varepsilon)P_{LO}B_e \tag{8}$$

$$\sigma_{LO-RIN}^2 = 2R_s^2\alpha^2(1-\varepsilon)^2P_{LO}^2RIN_sB_e \tag{9}$$

$$\sigma_{ASE}^2 = 2qR_s\alpha\varepsilon n_{sp}h\nu_s(G-1)B_eB_o \tag{10}$$

$$\sigma_{S-ASE}^2 = 4R_s^2\alpha^2\varepsilon^2GP_sn_{sp}h\nu_s(G-1)B_e \tag{11}$$

$$\sigma_{LO-ASE}^2 = 4R_s^2\alpha^2(1-\varepsilon)P_{LO}\varepsilon n_{sp}h\nu_s(G-1)B_e \tag{12}$$

$$\sigma_{ASE-ASE}^2 = 2R_s^2\alpha^2\varepsilon^2n_{sp}^2(h\nu_s)^2(G-1)^2B_eB_o, \tag{13}$$

where k_B is the Boltzmann constant, T is the temperature, F_{det} is the photodetector circuit noise figure, R_L is the photodetector load resistor, B_e is the electrical bandwidth, B_o is the

#233505 - $15.00 USD Received 29 Jan 2015; revised 24 Mar 2015; accepted 30 Mar 2015; published 8 May 2015

optical bandwidth, q is the electron charge, RIN_s is the relative intensity noise of the LO laser source, n_{sp} is the erbium-doped fiber amplifier (EDFA) population inversion factor, h is Planck's constant and ν_s is the signal optical frequency. It is assumed that $B_o \gg B_e/2$, the ASE spectrum is constant within B_o and the RIN spectrum is constant within B_e.

Similarly, we define the PCR also via a two-port input-output relation as we focus on a two-mode pump-degenerate FOPA. To model such a device we employ a semi-classical approach which treats signals as complex optical fields. The approach is valid as long as the large-photon-number assumption is satisfied [23, 24] and gives us the input-output relation as

$$\begin{bmatrix} E_{out,s} \\ E^*_{out,i} \end{bmatrix} = \begin{bmatrix} \mu & \nu \\ \nu^* & \mu^* \end{bmatrix} \begin{bmatrix} E_s \\ E^*_i \end{bmatrix}, \tag{14}$$

where E_s is the input signal complex optical field, E_i is the complex optical field of the second input mode conventionally known as the idler, $E_{out,s}$ denotes the output optical field of the signal, $E_{out,i}$ stands for the output optical field of the idler and $(*)$ represents the complex conjugate. Matrix coefficients μ and ν reflect the medium and the pump properties such as power and nonlinear interaction strength [23] and they satisfy the relation $|\mu|^2 - |\nu|^2 = 1$. The pump power is considered constant (undepletable), i.e., both signals are sufficiently small in power compared to the pump. It is customary to define a phase-insensitive gain as $G = |\mu|^2$ which implies $|\nu|^2 = G - 1$. For illustration purposes we use the same symbol G for both receivers but readers should keep in mind that in the SCR case it represents the preamplification and in the PCR case it constitutes the inherent amplification of the coherent mixer. The powers of the output modes are given by

$$P_{out,s} = |E_{out,s}|^2 = GP_s + (G-1)P_i + 2[G(G-1)P_sP_i]^{1/2}\cos\Delta\varphi_{PCR}, \tag{15}$$

$$P_{out,i} = |E_{out,i}|^2 = (G-1)P_s + GP_i + 2[G(G-1)P_sP_i]^{1/2}\cos\Delta\varphi_{PCR}, \tag{16}$$

where $P_s = |E_s|^2$ and $P_i = |E_i|^2$. Phase-sensitive operation is expressed through $\Delta\varphi_{PCR} = \varphi_\mu - \varphi_\nu - \varphi_s - \varphi_i$ where φ_μ and φ_ν are the phase angles of the complex matrix coefficients, φ_s is the phase angle of the input signal and φ_i is the phase angle of the input idler. Again, for the following discussion we assume that the two modes and the pump are phase-locked, $\Delta\varphi_{PCR} = 0$.

Equations (1) and (14) and Fig. 1 show graphically how we define the concept. The signal mode is the received signal and the idler mode is the LO (a CW signal), $E_i = E_{LO}$. Using the same definition from Eq. (4) the SNR of the PCR idler mode is defined as

$$SNR_{PCR} = \frac{4R_i^2\alpha^2 G(G-1)P_sP_i}{\sigma^2_{PCR}}, \tag{17}$$

and

$$\begin{aligned}\sigma^2_{PCR} = {} & \sigma^2_{det} + \sigma^2_i + \sigma^2_{AQN} + \sigma^2_{i-RIN} + \sigma^2_{i-PTN} + \sigma^2_{i-AQNi} \\ & + \sigma^2_{i-AQNs} + \sigma^2_{AQNi-AQNi} + \sigma^2_{AQNi-AQNs},\end{aligned} \tag{18}$$

where R_i is the photodetector responsivity at the idler frequency, σ^2_i is the idler shot noise variance, σ^2_{AQN} is the amplified quantum noise (AQN) shot noise variance, σ^2_{i-RIN} is the idler RIN variance and σ^2_{i-PTN} is the idler pump transferred noise (PTN) variance. The beating variances are defined between the idler and the idler AQN, σ^2_{i-AQNi}, the idler and the signal AQN, σ^2_{i-AQNs}, the idler AQN and the idler AQN, $\sigma^2_{AQNi-AQNi}$, and the idler AQN and the signal AQN, $\sigma^2_{AQNi-AQNs}$. The semi-classical approach allows us to treat the quantum noise (QN), also known as zero-point vacuum fluctuations, as an additive Gaussian noise [24] with a zero mean value

#233505 - $15.00 USD Received 29 Jan 2015; revised 24 Mar 2015; accepted 30 Mar 2015; published 8 May 2015

and the variance of $h\nu/2$, where ν is the optical frequency. The definitions of variances are based on studies by Kylemark *et al.* [25, 26] and are as follows:

$$\sigma_i^2 = 2qR_i\alpha P_{out,i}B_e \tag{19}$$

$$\sigma_{AQN}^2 = qR_i\alpha h\Big(\nu_s G + \nu_i(G-1)\Big)B_o B_e \tag{20}$$

$$\sigma_{i-RIN}^2 = 2R_i^2\alpha^2 P_{out,i}^2 RIN_i B_e \tag{21}$$

$$\sigma_{i-PTN}^2 = 4R_i^2\alpha^2 \frac{P_{pump}^2}{B_{res}OSNR_{pump}} P_i^2 \Big(\frac{dG}{dP_{pump}}\Big)^2 B_e \tag{22}$$

$$\sigma_{i-AQNi}^2 = 2R_i^2\alpha^2 P_{out,i}h\nu_i(G-1)B_e \tag{23}$$

$$\sigma_{i-AQNs}^2 = 2R_i^2\alpha^2 P_{out,i}h\nu_s G B_e \tag{24}$$

$$\sigma_{AQNi-AQNi}^2 = R_i^2\alpha^2(h\nu_i)^2(G-1)^2 B_e B_o \tag{25}$$

$$\sigma_{AQNi-AQNs}^2 = R_i^2\alpha^2 h^2\nu_s\nu_i G(G-1)B_e B_o, \tag{26}$$

where RIN_i is the relative intensity noise of the idler laser source, P_{pump} is the pump power, $OSNR_{pump}$ is the pump OSNR, B_{res} is the optical frequency bandwidth of 0.1 nm and ν_i is the idler optical frequency. The RIN spectrum and B_o assumptions from Eqs. (6)–(13) are considered as well. The AQN spectrum is assumed constant within B_o. Regarding the PTN variance, σ_{i-PTN}^2, the pump power distribution is assumed Gaussian and the noise is primarily determined by the pump and its ASE beating [26].

Equations (2)–(3), (6)–(13), (15)–(16) and (19)–(26) reveal basic differences between the two approaches. First, in the PCR case both waves and all the noise components beat within the FOPA all-optically while in the SCR case they beat during the process of photodetection. Second, the SCR mixer outputs are complementary (out of phase by π), i.e., if one output experiences constructive interference the second one experiences destructive one. Such behavior is the cornerstone of balanced detectors where both outputs are detected and subsequently processed differentially in electrical domain [10]. During this process, correlated components from both detectors are added coherently, independent noise components are added incoherently and the RIN of an LO is subtracted. In case of a FOPA we can control the properties of its output modes through their input phase relations which allows us to go from a coherent amplification (energy transfer from the pump onto modes and constructive interference between modes) to a coherent de-amplification (energy transfer reversed and destructive interference), however, all output modes acquire the same type of interference. Therefore the classic balanced detection using a single parametric mixer is not feasible and we focus on the fundamental single-ended option. Third, owing to its parametric nature the PCR requires an additional optical wave, the pump. Since a pump is required by all-optical preamplifiers in general, we treat it as an inherent property of the concept and do not consider it for the comparison. It is worth reminding that the PCR demands a pump which is phase-locked with both input waves. The same approach is utilized, for instance, in preamplifiers based on a phase-sensitive amplifier [27].

Even though the presented concept exploits the phase-sensitive regime of the FOPA (coherent amplification), it does not provide low-noise performance and phase-sensitive gain to such an extent as in other applications [14]. A low-noise operation is feasible when both input modes carry the same information and is most efficient when they are equal in power [19]. The concept violates both conditions, $P_i \gg P_s$ and the idler is CW, thus noise properties are similar to the FOPA in the phase-insensitive regime.

#233505 - $15.00 USD Received 29 Jan 2015; revised 24 Mar 2015; accepted 30 Mar 2015; published 8 May 2015

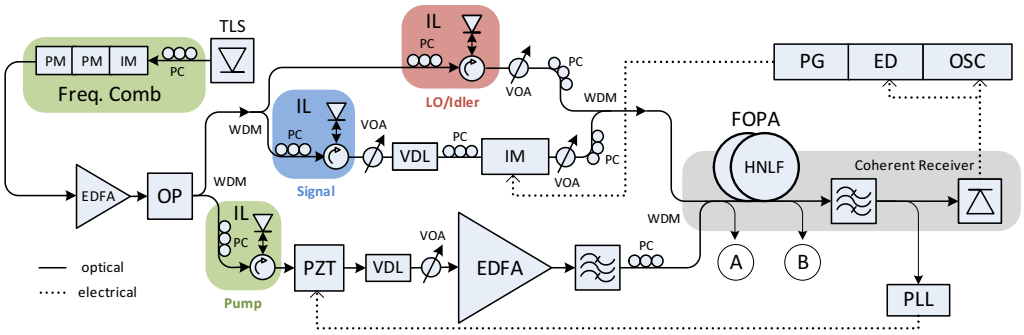

Fig. 2. Parametric coherent receiver set-up. TLS: Tunable laser source, IM: Mach-Zehnder intensity modulator, PM: phase modulator, EDFA: erbium-doped fiber amplifier, OP: optical processor, IL: injection locking, FOPA: fiber optical parametric amplifier, HNLF: highly nonlinear fiber, PC: polarization controller, VOA: variable optical attenuator), PLL: phase-locked loop), PZT: piezoelectric transducer, VDL: variable delay line, WDM: wavelength division (de)multiplexer, PG: pattern generator, ED: error detector, OSC: oscilloscope.

3. Experimental results

Figure 2 shows the experimental set-up used for the PCR analysis. The receiver requires phase-locked triplet (the pump, the signal and the idler constituting the LO) which we generate using a frequency comb. The comb comprises a cascade of a Mach-Zehnder intensity modulator (IM) and two phase modulators (PM) all driven by 25 GHz sinusoidal waveform. The cascade is seeded by a tunable laser source (TLS) at wavelength of 1554 nm and all output lines are boosted by an EDFA. We pick the triplet from the comb lines by means of a liquid-crystal-based optical processor (OP) where the wavelength of the pump is 1554 nm, the signal is 1550 nm and the idler is 1558 nm. Then they are split into separate arms via cascade of two wavelength division (de)multiplexers (WDM) of 200 GHz bandwidth and centered first at 1554 nm (separation of the pump) and second at 1549.7 nm (separation of the signal from the idler). We require all three waves to have a high OSNR and a high power therefore we employ a bank of slave lasers (distributed feedback lasers, $RIN = -150$ dB/Hz) to perform injection-locking (IL) technique. The pump undergoes boosting in high-power EDFA and its excessive ASE is filtered out by a 1 nm bandpass filter. Subsequently it is coupled to the FOPA through the WDM. The signal is modulated in the IM which is driven by a pattern generator (PG) with pseudorandom binary sequence of length of $2^7 - 1$ at 10 Gb/s. The modulation formats, OOK and BPSK, are selected through a tuning of the driving voltage and the bias of the IM. Both the signal and the idler are coupled via the WDM into the FOPA and their optical powers are controlled through variable optical attenuators (VOA). Using polarization controllers (PC) all three waves are launched co-polarized. The FOPA consists of four strained highly nonlinear fibers (HNLF) interconnected with isolators to suppress the stimulated Brillouin scattering (SBS) [28]. The HNLF cascade is 600 m long and has nonlinear coefficient of 10 $W^{-1}km^{-1}$ and average zero-dispersion wavelength of 1544 nm. For monitoring purposes both ends of the FOPA have optical couplers with 20 dB ratio. The coupler at the input of the FOPA is the point (label A) where the received signal power, P_s, and the idler/LO power, P_{LO}, are measured using an optical spectrum analyzer (OSA). After the pump is rejected through the WDM at the output of the FOPA, the idler (or optionally the signal) is additionally filtered via the WDM ($B_o = 200$ GHz) and detected in the PIN photodiode ($R_s = R_i = 0.88$ A/W, $F_{det} = 7$ dB, $R_L = 50\ \Omega$, band-pass filter $B_e = 7.5$ GHz). The FOPA and the photodetector represent the PCR. The additional loss between them, α, is 5 dB. Due to a phase-sensitive nature of the concept, temperature and mechanical perturbations

#233505 - $15.00 USD Received 29 Jan 2015; revised 24 Mar 2015; accepted 30 Mar 2015; published 8 May 2015

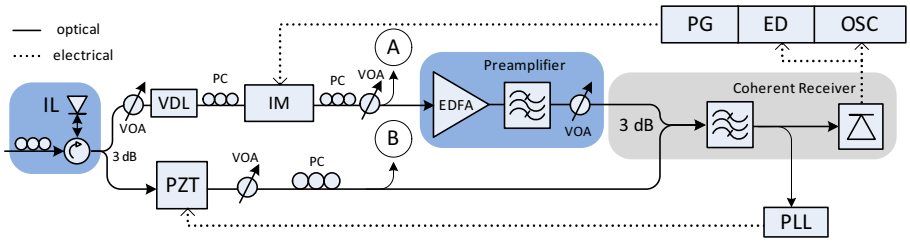

Fig. 3. Standard homodyne coherent receiver set-up. IL: injection locking, IM: Mach-Zehnder intensity modulator, EDFA: erbium-doped fiber amplifier, PC: polarization controller, VOA: variable optical attenuator), PLL: phase-locked loop), PZT: piezoelectric transducer, VDL: variable delay line, PG: pattern generator, ED: error detector, OSC: oscilloscope.

are taken care of by employing a phase-locked loop (PLL). The PLL uses the output signal tap and drives the piezoelectric transducer (PZT) located in the pump arm. As we study two modulation formats, OOK and BPSK, electrical front-end of the PLL was specifically designed for each of them. In case of OOK we detect feedback signal through a low-speed photodetector and in case of BPSK we implement recently presented scheme based on a high-speed photodetector and an envelope detector [29].

The experimental set-up of the SCR is shown in Fig. 3. For a fair comparison of both concepts we maintain set-up aspects and measurement conditions similar and consistent. The injection-locked slave laser used in the PCR set-up in the signal arm (see Fig. 2) acts as a source of frequency-locked pair - the signal and the LO (split via a 3 dB coupler). The signal is modulated in the same way as in the PCR set-up and coupled back together with the LO arm through a 3 dB coupler ($\varepsilon = 0.5$). To analyze the situation with and without preamplification the set-up is extended with a preamplifier which comprises an EDFA (noise figure of 4.8 dB), a 1 nm optical tunable filter (to suppress the ASE) and a VOA for acquiring a specific net gain. Both the signal and the LO are co-polarized via PCs and optical powers are adjusted through VOAs. The phase relation between both signals is maintained stable using the same PLL system whereas the PZT is placed into the LO arm. The output of the second 3 dB coupler is connected to the same final photodetection part as in the PCR set-up (with the same loss of 5 dB). To monitor the received signal power P_s (label A), and the LO power P_{LO} (label B), we tap out both arms via 20 dB couplers. The 3 dB coupler and the photodetector represent the SCR.

During the measurements we perform BER tests of the PCR concept using a single-quadrature non-return-to-zero (NRZ) BPSK or OOK format at a bit rate of 10 Gb/s. We also carry out the calculation of the BER defined as a function of the quality factor Q, $BER = \frac{1}{2}\mathrm{erfc}(Q/\sqrt{2})$, where erfc stands for complementary error function. The Q values for both modulation formats, derived from the SNR definitions (Section 2), are as follows: $Q_{BPSK} \approx SNR^{1/2}$ and $Q_{OOK} \approx (SNR/2)^{1/2}$. We would like to emphasize again that in the SCR case the gain G represents the signal preamplifier gain and in the PCR case it stands for the FOPA phase-insensitive net gain.

When we analyze the PCR we focus on the output idler mode, i.e., the CW at the input of the FOPA. The detection of the output signal mode offers similar performance with a negligible difference as was confirmed during our measurements. We present the PCR sensitivity measurement with BPSK signal, shown in Fig. 4, and as a reference we include the performance of the SCR without the preamplifier ($G = 1$). In the PCR case the net gain of the FOPA is kept low at 3 dB (tuned by pump power; $P_{pump} = 27.2$ dBm, $OSNR_{pump} = 57$ dB). The experimental results show approximately 9 dB sensitivity improvement over the SCR without the

#233505 - $15.00 USD Received 29 Jan 2015; revised 24 Mar 2015; accepted 30 Mar 2015; published 8 May 2015

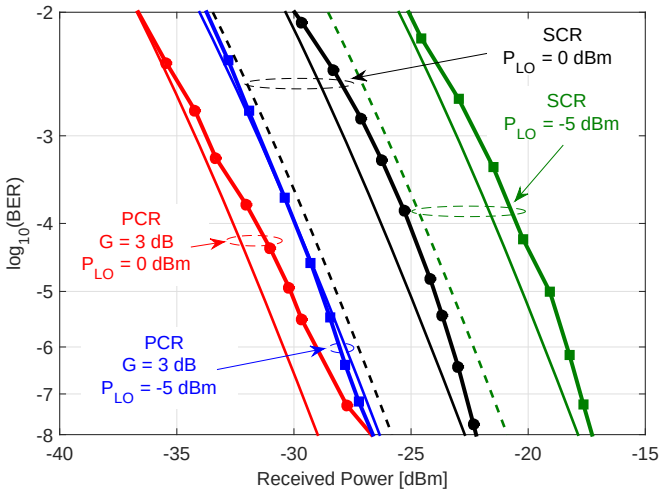

Fig. 4. Sensitivity measurements of BPSK signal at 10 Gb/s. Performance of the PCR (red and blue, $G = 3$ dB) and the SCR (black and green, without preamplifier) when the LO power is 0 dBm (circles) and -5 dBm (squares). Solid lines without symbols are respective numerical curves (both PCR and SCR) and dashed lines are respective numerical curves for the balanced SCR.

preamplifier in situation when the LO power is -5 dBm. This is the direct consequence of the gain in the PCR and the loss in the SCR. Moving to higher LO power of 0 dBm one can notice lower improvement for the PCR which is caused by the fact that the performance starts to be PTN- and RIN-limited.

In Fig. 5 we show the PCR performance with higher gain and the preamplification of the SCR input signal applied. For both receivers we set the LO power to -10 dBm and their gains are first fixed at the same value of 13 dB. For the FOPA this is near the maximum net gain we can achieve without suffering penalties from the SBS (P_{pump} = 29.2 dBm, $OSNR_{pump} = 57$ dB). The PCR gives a better performance than the single-ended SCR by approximately 13 dB. Under such conditions the PCR performance is limited mainly by the PTN and the SCR performance is still photodetector circuit noise-limited. It is worth pointing out that the noticeable difference between the measured and the numerical curves for the SCR case with the preamplifier is partially caused by not taking the loss between the preamplifier and the mixer into account. By increasing the SCR preamplifier gain to 33 dB we obtain the best performance limited by the signal-ASE beating, however, the same beating is also responsible for the performance floor when $BER < 10^{-4}$. For illustration purposes we show the calculated PCR sensitivity (magenta solid curve in Fig. 5) for a situation where the FOPA gain is also 33 dB but the LO power is reduced to -30 dBm. Under these conditions the PCR performance is idler-idler AQN beating-limited. Regarding the PCR numerical curves, values of the derivative term in Eq. (22) are acquired from a measurement of the FOPA pump power versus gain dependence and a subsequent extraction of differential values around selected gain values. The PCR curve when $G = 33$ dB is calculated using an extrapolation of the dependence when both the derivative terms and the pump power are obtained.

Both Figs. 4 and 5 also show numerical curves for the SCR case in the balanced configuration. Figure 5 portrays the situation when the performances of the single-ended and the balanced configurations converge as the received signal changes from photodetector circuit noise-limited

#233505 - $15.00 USD Received 29 Jan 2015; revised 24 Mar 2015; accepted 30 Mar 2015; published 8 May 2015

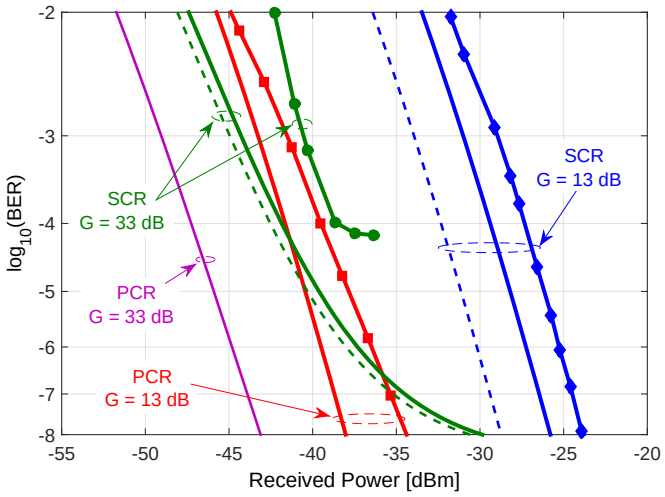

Fig. 5. Sensitivity measurements of BPSK signal at 10 Gb/s. Comparison of the PCR (red, $G = 13$ dB) and the SCR (blue, $G = 13$ dB, and green, $G = 33$ dB) when the LO power is -10 dBm. Solid lines without symbols are respective numerical curves (both PCR and SCR) and dashed lines are respective numerical curves for the balanced SCR. Magenta solid curve depicts the numerical performance of the parametric receiver with gain of 33 dB and -30 dBm LO power.

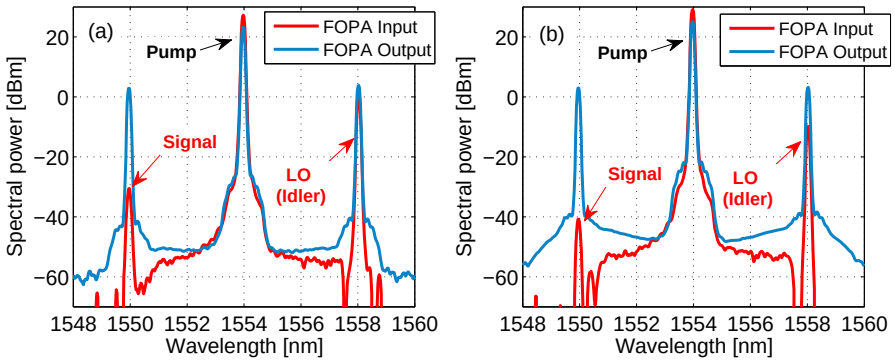

Fig. 6. Input and output spectra of the FOPA employed in the concept of parametric receiver: (a) $G = 3$ dB, $P_s = -30$ dBm, $P_{LO} = 0$ dBm and (b) $G = 13$ dB, $P_s = -40$ dBm, $P_{LO} = -10$ dBm.

(blue curves) to signal-ASE beating-limited (green curves).

The spectra of the input (label A in Fig. 3) and the output (label B in Fig. 3) of the FOPA depicted in Fig. 6 give an illustrative view on the coherent mixing process of spectrally distant signals and on FOPA-induced PTN and AQN. Two specific cases are portrayed. The low-gain case, $G = 3$ dB, $P_s = -30$ dBm, $P_{LO} = 0$ dBm, when the most prominent noise is the PTN observable around both output waves is shown in Fig. 6(a). The second case when the gain is high, $G = 13$ dB, $P_s = -40$ dBm, $P_{LO} = -10$ dBm, is shown in Fig. 6(b) which reveals the onset of the AQN apparent as an increased background noise. Readers should not be confused by unequal differences between the signal and the LO (the idler) at the input and at the output

#233505 - $15.00 USD Received 29 Jan 2015; revised 24 Mar 2015; accepted 30 Mar 2015; published 8 May 2015

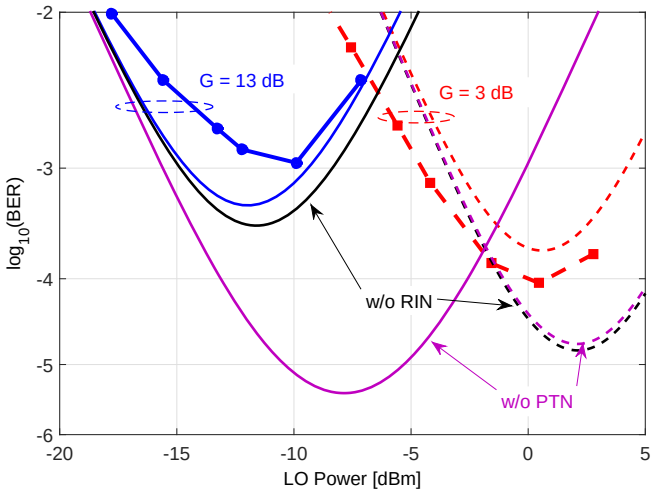

Fig. 7. Parametric receiver sensitivity measurements of OOK signal at 10 Gb/s when the LO power is varied. Dashed curves depict situation when $G = 3$ dB, $P_S = -30$ dBm, $P_{LO} = 0$ dBm and solid curves when $G = 13$ dB, $P_s = -40$ dBm, $P_{LO} = -10$ dBm. Experimental (square and circle markers), respective numerical curves (red and blue smooth curves) and numerical curves without the PTN (magenta) and without the RIN (black) are shown.

of the FOPA. The FOPA gain, G, is graphically noticeable (its magnitude) when comparing the input and the output idler (LO) spectral powers. The signal increase between the input and the output which exceeds 30 dB in Fig. 6(a) or 40 dB in Fig. 6(b) arises from the FOPA amplification as the energy is re-distributed between both modes [20].

In general, coherent receivers require a high-quality laser sources for the LO as the RIN can become a limiting factor of the sensitivity performance. In such situation noise fluctuations of the LO start to dominate and as they are approaching the levels of the received signal they deteriorate its SNR. In case of the PCR the situation is more complex as the PTN is present. Figure 7 shows the PCR sensitivity performance of an OOK signal while the LO is varied, the signal input power is kept constant and the FOPA has two different gains, 3 and 13 dB. It shows how both the effects considerably degrade the performance when reaching certain LO power level. To underline the magnitudes of their effects we numerically show the contributions of both the PTN and the RIN to the overall sensitivity performance. It can be seen that the PTN influence is substantial which leads to a conclusion that PCRs require a high-quality laser sources (i.e., with low RIN and high OSNR) for both the LO and the pump.

4. Discussion

In Section 2 we discussed the balanced detection option for the parametric receiver or more precisely its inapplicability due to specific properties of the FOPA output modes. To offer the balanced detection it would require two parallel FOPAs having the same gain (optionally increased to overcome the signal and the LO splitting losses) and adjusted phase-locking conditions (via a PLL system), $\Delta\varphi_{PCR} = \pi$ in Eq. (16). Such a solution would provide output modes out of phase by π at each FOPA which would be subsequently subtracted (after the photodetection), offering improved power dynamic range as in standard balanced receivers [10].

Another approach that is utilized in coherent systems in order to detect both-quadrature modulation formats (such as a quadrature phase-shift keying, QPSK) is the phase diversity, a simple

#233505 - $15.00 USD Received 29 Jan 2015; revised 24 Mar 2015; accepted 30 Mar 2015; published 8 May 2015

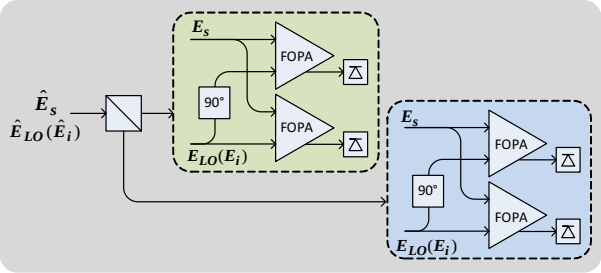

Fig. 8. Parametric coherent receiver with polarization and phase diversity scheme.

scheme where the signal and the LO are split and launched into two coherent receivers with LOs shifted in phase by 90°. Implementation in case of parametric receiver would again simply include two parallel FOPAs. To extend the scheme in order to cover both orthogonal polarization states (so-called polarization diversity [12, 22]) two parallel phase diverse schemes can be employed (split done by a polarization beam splitter) as is schematically shown in Fig. 8.

Homodyne coherent transmission systems based on co-propagation of signal and LO employ polarization-division multiplexing, i.e, they use orthogonal polarizations [4, 5]. The presented concept introduces a wavelength-division multiplexing option. In both cases the channel occupied by the LO can not be allocated for data transmission, however, in parametric case the LO wavelength can be placed to regions outside of conventional transmission windows defined primarily by EDFA gain profiles. This leaves certain channels LO-free and available for data transmission. In addition, only a single FOPA can preamplify and coherently mix several data channels with their respective LOs simultaneously. What must be taken into account is the fact that the parametric concept requires co-propagation of phase-locked waves therefore for transmission systems a dispersion compensation is needed. Moreover, a special treatment of the pump is also necessary. The solution how to overcome adverse nonlinear effects caused by a high-power pump propagating through a fiber resides in an attenuation of the pump before the link and its recovery at the end of the link by implementing an injection-locking based system [30].

Our experimental set-up relies on the phase-locked triplet generated in a frequency comb based on electro-optic modulators where the bandwidth is limited to ranges from few to tens of nanometers with the line spacing not exceeding tens of GHz. In order to acquire highly coherent frequency comb with both parameters greatly extended, a parametric shock wave mixer [31] offers a viable solution how to achieve bandwidths over 100 nm with hundreds of GHz line spacing. Technique how to create the triplet stretching over several hundreds of nanometers can harness a phase-preserving wavelength conversion of parametric translators [17]. Although translation does not provide desired gain as the efficiency is below 100 %, the phase-preserving capability promises a parametric coherent mixing of both modes. On the other hand, satisfying phase-matching conditions requires advanced dispersion control [17] and maintaining the triplet phase-locked can become a challenging task. Regardless of technical difficulties the presented concept can prove itself beneficial not solely to transmission systems but also to applications demanding high sensitivities such as sensing.

5. Conclusion

We presented the parametric coherent receiver based on a two-mode pump-degenerate FOPA. In a proof-of-concept experiment we verified the sensitivity performance at 10 Gb/s and discussed the main sources of additional penalties. The receiver is inherently single-ended and its key

#233505 - $15.00 USD Received 29 Jan 2015; revised 24 Mar 2015; accepted 30 Mar 2015; published 8 May 2015

benefit is the simultaneous optical preamplification and coherent mixing of the received signal and the LO which can be arbitrarily separated in wavelength.

Acknowledgments

Authors would like to acknowledge Pontus Johannisson and Magnus Karlsson for fruitful discussions on coherent detection. Lan Liu is acknowledged for useful comments on the PLL system. This work is supported by the European Research Council under grant agreement ERC-2011-AdG - 291618 PSOPA and by the K. A. Wallenberg Foundation.

#233505 - $15.00 USD Received 29 Jan 2015; revised 24 Mar 2015; accepted 30 Mar 2015; published 8 May 2015